Volume 14 | Number 4 | 21 February 2014 | Pages 611–816

Lab on a Chip

Miniaturisation for chemistry, physics, biology, materials science and bioengineering

www.rsc.org/loc

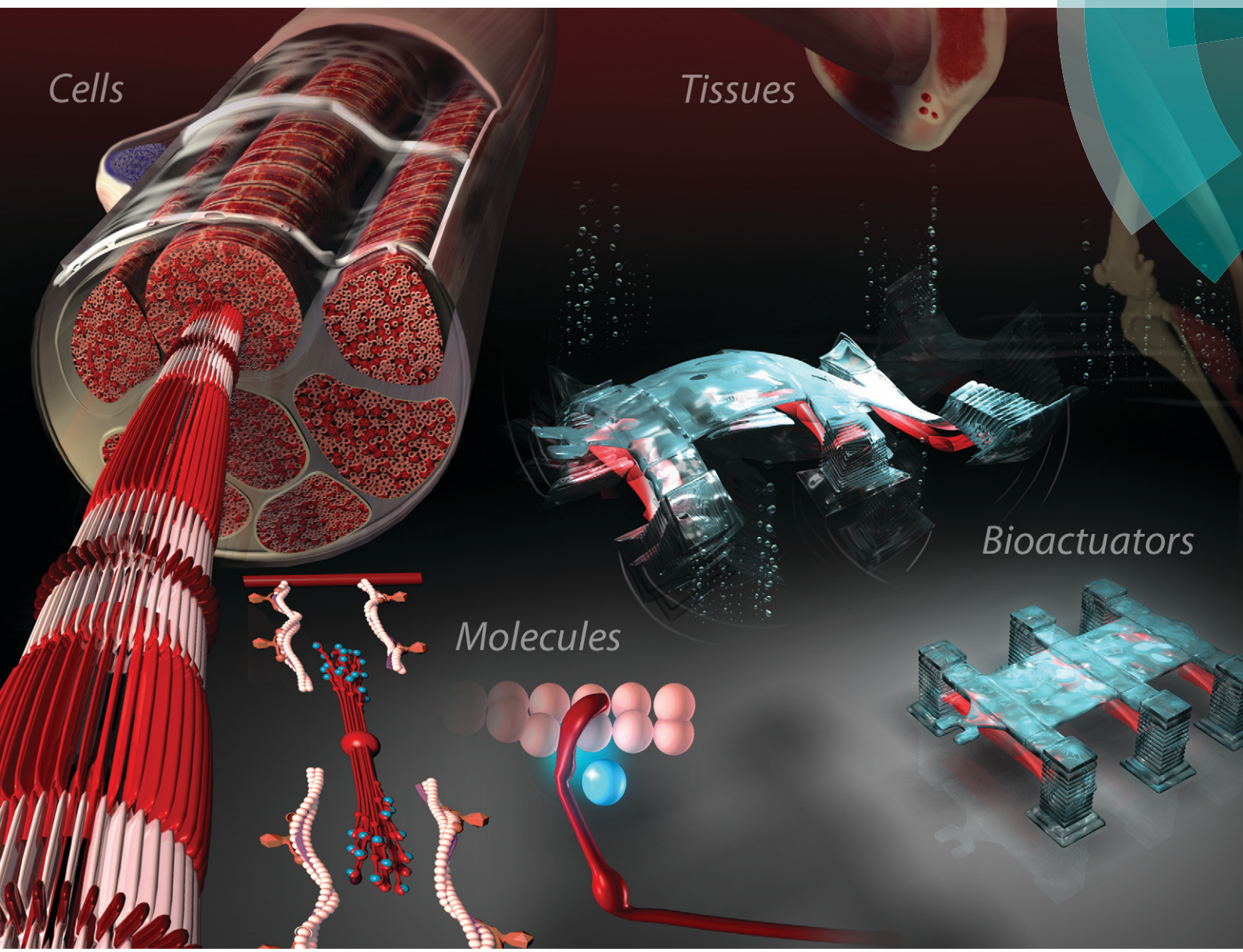

ISSN 1473-0197

ROYAL SOCIETY OF CHEMISTRY

CRITICAL REVIEW

Rashid Bashir *et al.*

Utilization and control of bioactuators across multiple length scales

Lab on a Chip

CRITICAL REVIEW

Utilization and control of bioactuators across multiple length scales

Cite this: *Lab Chip*, 2014, **14**, 653

Vincent Chan,[a] H. Harry Asada[a] and Rashid Bashir*[b]

In this review, we summarize the recent developments in the emerging field of bioactuators across a multitude of length scales. First, we discuss the use and control of biomolecules as nanoscale actuators. Molecular motors, such as DNA, kinesin, myosin, and F_1-ATPase, have been shown to exert forces in the range between 1 pN to 45 pN. Second, we discuss the use and control of single and small clusters of cells to power microscale devices. Microorganisms, such as flagellated bacteria, protozoa, and algae, can naturally swim at speeds between 20 μm s^{-1} to 2 mm s^{-1} and produce thrust forces between 0.3 pN to 200 pN. Individual and clustered mammalian cells, such as cardiac and skeletal cells, can produce even higher contractile forces between 80 nN to 3.5 μN. Finally, we discuss the use and control of 2D- and 3D-assembled muscle tissues and muscle tissue explants as bioactuators to power devices. Depending on the size, composition, and organization of these hierarchical tissue constructs, contractile forces have been demonstrated to produce between 25 μN to 1.18 mN.

Received 28th August 2013,
Accepted 27th November 2013

DOI: 10.1039/c3lc50989c

www.rsc.org/loc

Introduction

Nature has long been a source of inspiration in producing complex yet elegant functional systems and life forms across a multitude of length scales.[1] Marcello Malpighi, one of the greatest seventeenth-century life scientists, was one of the first to attribute body function to an organized series of minute 'organic', or biological, machines.[2] The length scales of these biological machines span from the tiny machinery in cells that participate in replication (mitotic cell division) and locomotion (actin and myosin systems) to cell cluster interactions and formation of tissues having higher-order functionalities (or so-called emergent properties). In fact, the human body is a large and complex functional system – the ultimate biological machine.[3] Traditionally, the study of these systems has been the domain of biology, while technological advances have been used by biologists as new tools to advance these studies. This has resulted in a one-way relationship between biology and engineering. However, recent advances in cellular and molecular biology, combined with new technologies to measure and manipulate cell behavior, have laid the foundation for the next frontier in biology, that of creating our own engineered biological machines.[4]

[a] *Department of Mechanical Engineering, Massachusetts Institute of Technology, Cambridge, MA 02139, USA*
[b] *Department of Bioengineering, University of Illinois at Urbana-Champaign, Urbana, IL 61801, USA. E-mail: rbashir@illinois.edu*

Vincent Chan

Vincent Chan, PhD is a Research Scientist in the Mechanical Engineering Department at the Massachusetts Institute of Technology. He obtained his PhD in Bioengineering from the University of Illinois at Urbana-Champaign, MS in Biomedical Engineering from Purdue University, and BS in Biomedical Engineering from the Johns Hopkins University. His research interests focus on microscale and nanoscale technologies for cellular systems, tissue engineering, and regenerative medicine.

H. Harry Asada

H. Harry Asada, PhD is the Ford Professor of Engineering and Director of the Brit and Alex d'Arbeloff Laboratory for Information Systems and Technology in the Department of Mechanical Engineering at the Massachusetts Institute of Technology. His research programs have focused on design, system dynamic, and control of robotic, biomedical, and biological systems. He has published 3 books, 119 archival journal papers, and 369 refereed conference proceeding papers, and holds 25 US patents.

Over the past decade, extensive research has been conducted to exploit the use of bioactuators for engineering new biological machines.[5] A list of the functional performances of bioactuators across the molecular, cellular, and tissue scales are shown in Table 1. There are a number of attractive design features that make bioactuators unique in nature.[6] Bioactuators are different in composition from their man-made counterparts. Whereas man-made machines are traditionally constructed from hard and dry materials, such as metals, ceramics, and plastics, bioactuators are comprised of soft and wet materials, such as DNA, proteins, and cells. Typically, man-made actuators are powered by electrical energy that is transformed at low efficiency (<30%) to mechanical work and a resulting large heat loss. In contrast, bioactuators harvest chemical energy at much higher efficiencies (≥50%) than is possible from man-made actuators. Bioactuators are also capable of self-assembly. While their basic functional units, such as motor proteins, single cells, or microorganisms, can function independently, they exhibit collective behavior and can assemble into hierarchical structures. Examples of collective behaviors include motor proteins that are recruited to form multi-molecular assemblies, cardiac cells that establish electrical gap junctions for synchronous contraction, and microorganisms that swarm when in close proximity to each other. Furthermore, bioactuators are intrinsically programmed with a wide variety of control mechanisms that can be exploited. One commonly used control mechanism is electric field stimulation. It can be used to guide polarized microtubules on kinesin beds through microchannel junctions, steer galvanotactic swarmer cells to predetermined destination points, and stimulate contractile muscle tissue to twitch. It is even possible now to introduce other control mechanisms in bioactuators not seen in nature through new tools in synthetic biology and genetic engineering.

The potential benefits of utilizing and controlling the unique capabilities of nature's bioactuators across all length scales are enormous.[7] At the molecular scale (10^{-9} m), motor proteins can be used to develop *in vitro* sensors and bioassays. A small cluster of motor proteins such as kinesin can be used to capture, separate, and transport target analytes. This enables a high degree of miniaturization in closed devices and removes the need for mechanical pumping or electrokinetic-driven flow of target analytes. At the cellular scale (10^{-6} m), cells and microorganisms can be used as microrobots for *in vivo* diagnostic and therapeutic tasks, probing, analyzing, and transporting microobjects in biology, and microfluidic applications in lab-on-a-chip devices. One exemplary example is an autonomous microrobot that can carry out a complex sequence of tasks inside the circulatory system of the human body. These microrobots can be used for *in vivo* targeted drug delivery or even radiation therapy by placing radioactive seeds near unwanted cells or tumors. At the tissue scale (10^{-3} to 10^{-2} m), living muscles and muscle tissues can be used as continuum actuators for applications in soft robotics and surgical biobots. While traditional robots are constrained by joints with limited range of motion, living muscles have high degrees of freedom that can constantly bend along their length. One vision is the creation of biological robots, or biobots, that perform or assist in specific surgical procedures, such as sealing small blood vessels to minimize bleeding during surgery, repairing injured tendons, or targeting and eliminating metastatic tumors.[8]

In this review, we summarize the recent developments in the emerging field of bioactuators across a multitude of length scales. First, we discuss the use and control of biomolecules as nanoscale actuators. Molecular motors, such as DNA, kinesin, myosin, and F_1-ATPase, have been shown to exert forces in the range between 1 pN to 45 pN. Second, we discuss the use and control of single and small clusters of cells to power microscale devices. Microorganisms, such as flagellated bacteria, protozoa, and algae, can naturally swim at speeds between 20 μm s^{-1} to 2 mm s^{-1} and produce thrust forces between 0.3 pN to 200 pN. Individual and clustered mammalian cells, such as cardiac and skeletal cells, can produce even higher contractile forces between 80 nN to 3.5 μN. Finally, we discuss the use and control of 2D- and 3D-assembled muscle tissues and muscle tissue explants as bioactuators to power devices. Depending on the size, composition, and organization of these hierarchical tissue constructs, contractile forces have been demonstrated to produce between 25 μN to 1.18 mN.

Rashid Bashir

Rashid Bashir, PhD is the Abel Bliss Professor, Co-Director of the Center for Nanoscale Science and Technology, and Department Head of Bioengineering at the University of Illinois at Urbana-Champaign. His research programs have focused on BioMEMS, lab-on-a-chip, nanobiotechnology, interfacing biology and engineering from molecular to tissue scale, and applications in semiconductor fabrication to biomedical engineering. He has co-authored over 166 journal papers, 192 conference papers and abstracts, 119 invited talks, and has been granted 34 patents.

Biomolecular actuators

Biomolecular motors are considered promising materials for constructing biological actuators with piconewton (pN) forces.[9] In general, biomolecular actuators are driven by the conversion of adenosine triphosphate (ATP) to drive their movement. These actuators can be used in nanoscale mechanical devices to pump fluids, open and close valves,

Table 1 Forces, speeds, and step sizes of bioactuators. Measured and calculated forces, speeds, and step sizes cited in literature of engineered and natural bioactuators across multiple length scales

	References	Force, speed, and/or step size			Type of bioactuator
DNA	15	10–15	pN	Force, unzip	Hybridized DNA
	14,16	15–37	pN	Force, close/push	Nanoactuators
	21,23	0.7–3.0	nm min^{-1}	Speed	DNA walkers
	17,18,21,23	2–28	nm	Step size	DNA walkers
Kinesin–microtubules	30,35,36,46,48	5–8	pN	Force	Kinesin, *in vitro*
	28,32,33,34,35	0.25–0.5	μm s^{-1}	Speed	Kinesin, *in vitro* (natural assay)
	17,46,48	8	nm	Step size	Kinesin, *in vitro* (natural assay)
	27,31	0.11–2.3	μm s^{-1}	Speed, fast axonal	Kinesin, *in vivo*
	27	1.16–34.7	μm s^{-1}	Speed, slow axonal	Kinesin, *in vivo*
	35	0.38	μm s^{-1}	Speed	Dynein, *in vitro*
	36,40,42,44,45,46	0.50–0.75	μm s^{-1}	Speed	Microtubules, *in vitro* (inverted assay)
	36	15–30	nm	Step size	Microtubules, *in vitro* (inverted assay)
Myosin–actin	59,61	1.4–4.0	pN	Force	Myosin II, *in vitro* (not processive)
	60	5–15	nm	Step size	Myosin II, *in vitro* (not processive)
	58	10	nm	Step size	Myosin II, *in vivo*
	65	3	pN	Force	Myosin V, *in vitro* (not processive)
	60,64	0.2–0.45	μm s^{-1}	Speed	Myosin V, *in vitro* (not processive)
	60	36	nm	Step size	Myosin V, *in vitro* (not processive)
	60	1	μm s^{-1}	Speed, organelles	Myosin V, *in vivo*
F_1-ATPase	67,68	40–45	pN nm^{-1}	Force, torque	F_1-ATPase, *in vitro*
		45	pN	Force (near 100% eff.)	F_1-ATPase, assume 1 nm radius at β–γ interface
Bacteria	84	0.3–0.5	pN	Force, thrust	Flagellated bacterium (typical)
	80,84	20–100	μm s^{-1}	Speed	Flagellated bacterium (typical)
	76	0.5	pN	Force, thrust	*S. marcescens* (about 50), 10 μm bead
	76	4.7	μm s^{-1}	Speed	*S. marcescens* (about 50), 10 μm bead
	80	14.8	μm s^{-1}	Speed	*S. marcescens* (about 10), 10 μm unpatterned bead
	80	28.2	μm s^{-1}	Speed	*S. marcescens* (about 10), 10 μm patterned bead
	82	7	μm s^{-1}	Speed	*S. marcescens*, 50 μm × 100 μm rectangle
	83	9.15	μm s^{-1}	Speed	*S. marcescens*, 50 μm triangle
	80,82	0.45–0.48	pN	Force, thrust	*S. marcescens*, nature
	76,83	20–47	μm s^{-1}	Speed	*S. marcescens*, nature
	78	2–5	fN m^{-1}	Force, torque	*M. mobile*, rotor at 1.5–2.6 rpm
	78	0.18	fN m^{-1}	Force, torque	*M. mobile*, nature
	78	27	pN	Force, thrust	*M. mobile*, nature
	78	2–5	μm s^{-1}	Speed	*M. mobile*, nature
	84	4	pN	Force, thrust	MC-1, nature
	84	300	μm s^{-1}	Speed	MC-1, nature
	81	0.05	μm s^{-1}	Speed	*S. typhimurium*, 8 μm unpatterned bead
	81	0.37	μm s^{-1}	Speed	*S. typhimurium*, 8 μm patterned bead
Protozoa	85	2.0	mm s^{-1}	Speed	*P. caudatum*
	85,86	0.7–27	nN	Force, thrust	*P. caudatum*
	87	200	pN	Force, thrust	*T. pyriformis*
	87	786.7	μm s^{-1}	Speed	*T. pyriformis*
	88	40	pN	Force, thrust	*V. convallaria*
	88	8.8	cm s^{-1}	Speed, contractile	*V. convallaria*
	88	54	μm	Step size	*V. convallaria*
Algae	89	25.8	pN	Force, thrust	*C. reinhardtii*
	90	100–200	μm s^{-1}	Speed	*C. reinhardtii*
Single muscle cells	91	80	nN	Force	Cardiac cells, hydrogel-based micropillars
		3.5	μN	Force	Cardiac cells, PDMS-based micropillars
	92	1.01	μN	Force, tetanus	Skeletal cells, silicon cantilever
Natural and synthetic Tissues	93	25–600	μN	Force	Cardiac sheet, PDMS-based cantilevers
	94	20	μN	Force	Cardiac cluster, PDMS gear
	96	1.18	mN	Force	Cardiac sheet, 4 stacks
	99	38	μm s^{-1}	Speed	Cardiac walker (138 μm long, 40 μm wide)
		25	μm	Step size	Cardiac walker (138 μm long, 40 μm wide)
		77.28	μN	Force	Cardiac walker (138 μm long, 40 μm wide)
	100	140	μm s^{-1}	Speed	Cardiac walker (400 μm front leg, 1200 μm rear leg)
	101	133	μm s^{-1}	Speed	Cardiac swimmer (5 mm length)
		400	μm s^{-1}	Speed	Cardiac walker (5 mm length)
	104	236	μm s^{-1}	Speed	Cardiac walker (7 mm length)
		354	μm	Step size	Cardiac walker (7 mm length)

and provide translational movement of cargo.[10] The difficulty lies in how to integrate these sophisticated functions to do specific tasks. In the following section, we take a look at the current state of the field, from the *ex vivo* assembly of motor

proteins, such as DNA, kinesin–microtubules, actin–myosin, and F_1-ATPases, to the transport and external control of these nanoscale engineered systems for carrying out distinct functions.

DNA motor molecules

DNA is an attractive nanodevice because of its self-assembly properties. It has been shown previously that branched motifs of DNA can provide components for the assembly of nanoscale objects, links, and arrays.[11,12] However, switchable biomolecular machines can also be assembled with DNA. The basic concept of DNA as a biomolecular actuator is based on the fact that DNA can switch between two stable conformational states. These states can be controlled based on the ionic composition of the medium or the presence of complementary single-stranded molecules. There have been several successful demonstrations that harness this ability for the construction of biomolecular actuators. Here, we describe several different types of motion with DNA machines: (1) rotation, (2) extension and folding, and (3) walking.

To achieve a rotational motion, Mao *et al.* assembled a switchable molecular machine from synthetic DNA molecules.[13] The construct consisted of two rigid 'arms' of DNA that were rotated between fixed positions. The DNA arms consisted of 'double-crossover' (DX) molecules that linked to the long central DNA strand of 4.5 double-helical turns. The central strand had a base-paired sequence $d(CG)_{10}$, called a 'proto-Z' sequence that switched between the right-handed helical B-conformation and the left-handed Z-state at high ionic strength. When this conformational change occurred, the two DX-stabilized strands rotated around their longitudinal axes and twisted about 200° relative to each other. This event was able to induce atomic displacements of 20–60 Å.

To achieve a 'scissor-like' extension and folding motion, Yurke *et al.* exploited the ability of DNA hybridization as an energy source to power a pair of 'nano-tweezers' constructed from three DNA molecules.[14] The DNA molecules were constructed with a rigid, double-stranded region and two flexible, single-stranded dangling ends. When single-stranded DNA 'fuel' was added, they hybridized with the dangling ends to pull the tweezers closed. The mechanism of movement was a change in flexural persistence length upon hybridization, which altered the bending stiffness.[15] Complementary strands that compete for hybridization of the DNA fuel were then added to allow the tweezers to open. In similar fashion, Simmel *et al.* constructed a 'nano-actuator' with two strands of DNA that hybridized together to form a loop-like structure.[16] The structure had two rigid double-stranded arms held together by one short and one long single-stranded region. Upon hybridization, the DNA fuel pushed the arms apart into a straightened configuration. The nano-actuator was relaxed by adding complementary strands of the DNA fuel.

To achieve a walking motion, Shin and Pierce developed a very simple DNA walker based on hybridization and branch migration.[17] The walker consisted of a DNA duplex with two single-stranded feet. The track also consisted of a DNA duplex with branched single-stranded extensions as binding sites for the walker. The feet of the walker were attached to the track by linker molecules in the solution. One of the linker molecules was then removed by competitive binding to free the foot for the next binding site. This was repeated several times to move the walker distances of 5 nm per step. Omabegho *et al.* constructed an autonomous DNA bipedal walker that uses alternating DNA fuel strands to coordinate the action of its two legs.[18] This leads to a "burnt bridges" Brownian ratchet-type mechanism that irreversibly consumes the track as the DNA bipedal walker proceeds. Each step size in this autonomous walker design was about 28 nm. Other DNA walkers used gears[19] or enzymes[20,21] to facilitate unidirectional movement, but the overall mechanisms were similar.

Recently, DNA walkers have been developed with directional control by sensing and modifying the tracks laid out in front of them. Lund *et al.* reported a molecular 'spider' consisting of a streptavidin body with three DNAzyme catalytic legs that performed action sequences, such as 'start', 'follow', 'turn', and 'stop', on a DNA origami platform.[22,23] The step size was approximately 2 nm per cleavage step, and the rate of spider movement was about 3 nm min^{-1}. Muscat *et al.* reported a programmable and autonomous molecular robot fueled by DNA hybridization.[24] It consisted of tracks with road junctions that had DNA anchorages. The fuels contained destination information that moved the molecular robot forward using the DNA anchorages in a specified sequence. This represented the next generation in DNA walkers by demonstrating programmable branched tracks using encoded DNA.

Kinesin-microtubule linear motor proteins

Microtubules are intracellular filaments involved in many cell processes.[25] They are involved in forming the mitotic spindle during cell division, maintaining cell structure, providing platforms for transport, and locomotion. The main building blocks of microtubules are α- and β-tubulin, which spontaneously bind together to form heterodimers. These tubulin heterodimers assemble into linear protofilaments that make up the structure of microtubules. Microtubules are hollow tubes of 25 nm in diameter and consist of 13 protofilaments *in vivo*. They have polarity with the plus-end at the side that the β-tubulins point towards and the minus-end at the side that the α-tubulins point towards. Microtubules provide linear substrates that motor proteins, such as kinesin, can move along.

Kinesins are one class of motor proteins that use microtubules as a transport system for nanoscale cargo.[26,27] Kinesins consist of two motor 'head' domains that are connected to an α-helical neck by short, highly flexible neck linkers. The neck is connected to a linear stalk that has cargo binding sites at its 'tail'. Each head has two separate binding sites: one for the microtubule and the other for ATP.

Hydrolysis of ATP and subsequent ADP/P_i release changes the conformation of the microtubule-binding domain and the orientation of the neck linker that results in the walking motion of the kinesin. The walking motion proceeds in 8 nm steps using a 'hand-over-hand' mechanism that puts one motor domain before the other. The short neck linker is important for guiding the direction of movement of cargo. The linear stalk is important not only for binding cargo, but also for regulating motor activity. Without cargo, kinesin is turned off by self-inhibition.

It is not a trivial task to engineer microtubule transport systems *ex vivo*, particularly in versatile geometries with intersections and complex shapes. Turner *et al.* developed a natural microtubule motility assay by fixing microtubules onto glass substrates with either silane[28] or glutaraldehyde.[29] Kinesin-coated beads in a motility buffer were introduced, and bead movements were observed with time-lapse imaging. In order to achieve unidirectional movement, microtubules were oriented by anchoring the minus-end of microtubules.[30,31] Limberis *et al.* demonstrated immobilization of microtubules on a glass surface treated with VαNT1, an antibody that binds specifically to the minus-end of microtubules.[30] Polar alignment was achieved by applying fluid flow to the immobilized microtubules (>90% orientation). A wide range of cargo can be selectively transported on these highly-oriented microtubule railways, including quantum dots (10–20 nm diameter),[32] polystyrene beads (500 nm diameter),[31] oil droplets (5–20 μm),[33] and silicon particles (2 × 3 × 2 μm).[34]

A unique advantage of using the natural microtubule motility assay is the wide variety of anterograde/retrograde motors and natural adaptor proteins to sort and transport cargo toward either microtubule plus-ends or minus-ends. Yokokawa *et al.* demonstrated bi-directional transport by using kinesin- and dynein-coated microspheres on oriented microtubules.[35] However, the movement of kinesin and dynein on the microtubules are only one dimensional, and the cargo drops off once the end of the filament is reached. Furthermore, kinesin and dynein only makes a few hundred steps before dissociating from the microtubule. Consequently, Howard *et al.* demonstrated an inverted microtubule motility assay by immobilizing a bed of kinesin molecules on glass surfaces (Fig. 1A).[36] Microtubules were then perfused into the chamber and exhibited motility. Pivots around a single nodal point represented interaction of a microtubule with a single kinesin molecule. A number of track designs based on these inverted motility assays were fabricated to guide filaments efficiently.

Hiratsuka *et al.* reported the first milestone of unidirectional microtubule motion by using photolithography to fabricate micro-grooved tracks.[37] Since microtubules can still travel in opposite directions, unidirectional motion was achieved by sorting microtubules with asymmetric arrow-shaped features. Microtubules that wandered into these channels were forced to turn around. Similar topographical features, such as ratchets,[38] roundabouts,[39] and microchannels[40] have been studied for efficient unidirectional sorting.[41] The addition of overhanging walls was also particularly effective at preventing microtubule escape from the channels.[42] Yokokawa *et al.* used fluid flow to orient kinesin-propelled microtubules by removing the ones that glided upstream.[43] van den Heuvel *et al.* steered microtubules through Y-junction channels using active electrical control.[44] Electric fields were able to bias the direction of negatively-charged microtubules by bending the free leading tips toward the next kinesin motor. While the magnitude of the electric fields did not affect the speed of the microtubules (0.75 μm s^{-1}), it did change the average bending of the microtubule path. For cargo selection, the molecular recognition sites of microtubules have been engineered to allow desired cargo to be bound and transported. This is typically done by tagging the cargo with antibodies or biotinylating microtubules and coating cargo with avidin or streptavidin (Fig. 1B). Polymeric and magnetic beads,[45] gold nanoparticles,[46,47] DNA,[48,49] and viruses,[50,51] have all been coupled to microtubules through these linkages. Much larger cargos such as silicon needles have also been reported.[52] Furthermore, Hiyama *et al.* was the first to demonstrate autonomous loading and unloading of transported cargoes using DNA hybridization without external stimuli.[53,54] Cargo loading and unloading zones have been built for large-scale transport applications.[47,55] Passing microtubules collide with cargo, pick them up, and transport them into cargo-free areas (Fig. 1C).

Application-oriented bio-assays that integrate many of the aforementioned principles to capture, transport, and detect target proteins are now in early development. Carroll-Portillo *et al.* constructed kinesin 'nanoharvesters' using streptavidin-coated quantum dots that served as scaffolds for spatially-organized biotinylated kinesin and antibodies selective against TNF-α.[56] These nanoharvesters were introduced in solution and shown to move along microtubules bound to glass coverslips. Treatment with TNF-α and secondary detection quantum dots showed capture and transport. Fujimoto *et al.* microfabricated large parallel arrays of nanotracks optimized to orient the microtubules' polarity for bio-assays.[57] Again, streptavidin-coated quantum dots were employed as scaffolds for spatially-organized biotinylated N-kinesin (anterograde)–dynein (retrograde) and glutathione S-transferase (GST)–glutathione (GHT). The motility of N-kinesin and dynein in opposite directions on the same microtubules caused collisions that resulted in colocalization of the quantum dots and binding interaction of the GST–GHT conjugates. This demonstrated feasibility of a massively parallel bio-assay analysis tool.

Actin–myosin linear motor proteins

Actin is another type of cytoskeletal filament and is important in cell motility, cytokinesis, and cell attachment to substrates by focal adhesions.[58] In many ways, they resemble microtubules. Actin filaments have polarity because their

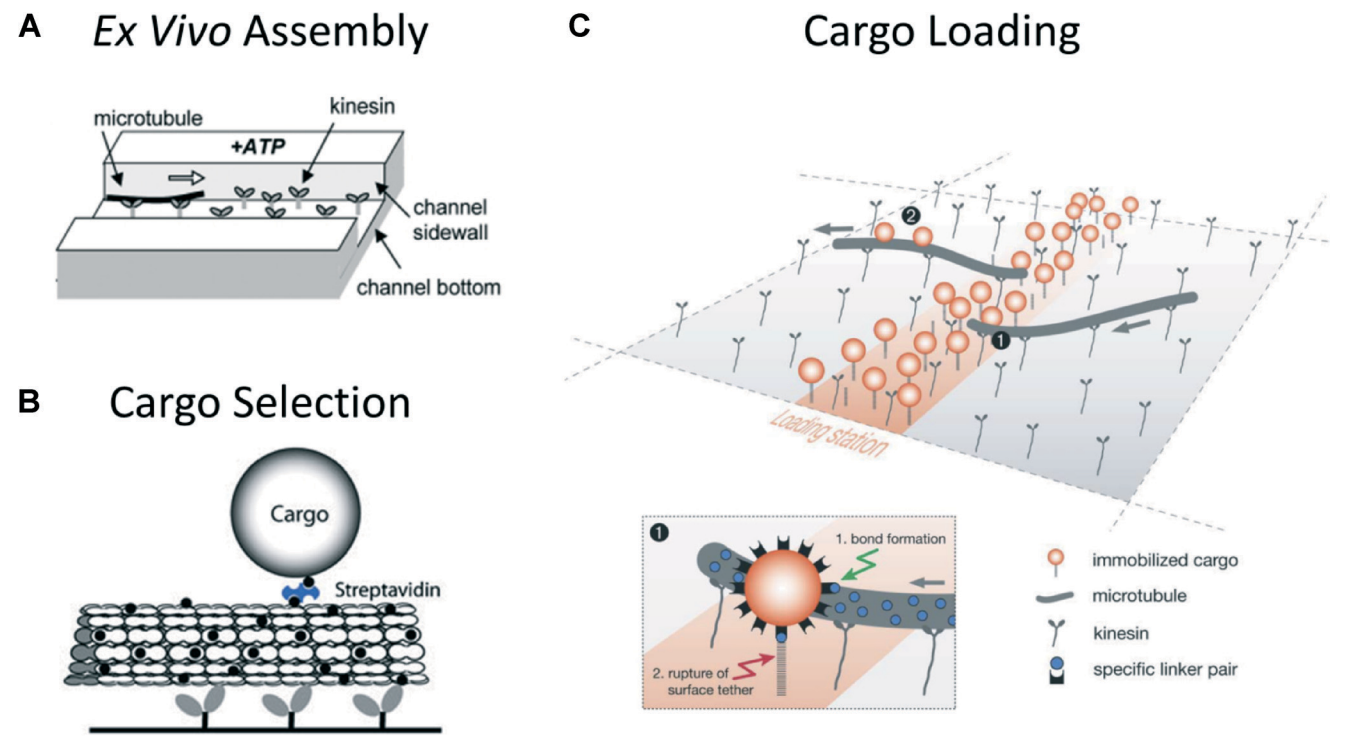

Fig. 1 Molecular-level biological machines. (A) A bed of kinesin molecules coated on to glass substrates can be used to guide microtubules along patterned tracks or microchannels [reprinted from ref. 39]. (B) Molecular recognition sites of microtubules have been engineered to allow desired cargo to be attached and transported. This is typically done by tagging the cargo with antibodies or biotinylating microtubules and coating cargo with avidin or streptavidin. (C) Cargo loading zones have been built for large-scale transport applications. Passing microtubules collide with cargo, pick them up, and transport them into cargo-free areas [reprinted from ref. 46].

monomers orient with their cleft toward the same end of the filament (plus-to-minus). Their monomers also spiral around the axis of the filament with a structure similar to a double helix. They are highly dynamic and can polymerize and depolymerize rapidly. Like kinesin, myosin molecules are a class of motor proteins that bind to actin, hydrolyze ATP, and move along the filaments. The most common type of myosin motor is myosin II, which generates between 1.4–3.5 pN of force.[59]

The technologically-motivated development of classical motility assays into devices for controlled microscale transport has not been as rapid in actomyosin systems as in the case of microtubule–kinesin. There are several reasons for this. The most widely available myosin is myosin II, which is not 'processive'.[60,61] This means that after one step (ATP hydrolysis that leads to a conformational change), the myosin detaches from the actin. This makes it almost impossible to transport cargo along actin filaments. However, there does exist variants of myosin that are processive (myosin V and VI).[62,63] *In vitro* experiments for myosin V produced mean velocities in the range of 0.2–0.45 nm s^{-1}.[64] It has a stall force of 3.0 ± 0.3 pN at 2 mM ATP, considerably less than the 5–8 pN observed for kinesin.[65] Presently, there have not been many reports of its use as a biological machine. Furthermore, the stiffness of actin is much less than the stiffness of microtubules. As a result, the filaments are 'floppy' and can maneuver around microfabricated structures easily.[66] Because of the helical structure of actin, myosin will follow a helical path when actin is attached to the substrate, or actin filaments gliding along a bed of myosin will rotate and eventually the cargo will inhibit its movement.

F_1-ATPase rotary motor proteins

To date, F_1-ATPase is probably the best understood biomolecular motor. Coupled with the membrane-embedded proton-conducting unit F_0, it forms the H^+-ATP synthase that reversibly couples transmembrane proton flow to ATP synthesis/hydrolysis in respiring and photosynthetic cells. F_1-ATPase consists of a hexamer stator of alternating α and β subunits. In the central cavity of the hexamer is a stalk rotor made up of γ, δ, and ε subunits. This γδε-subunit rotates in an anticlockwise direction within the αβ-subunit as it hydrolyses ATP.

Noji *et al.* first isolated and immobilized the F_1 complex on a glass surface by linking its histidine tags with Ni^{2+}–nitrilotriacetic acid (Ni–NTA).[67] Fluorescently-labeled actin filaments were attached to the γδε-subunits to visualize its rotation directly. In the presence of ATP, the filaments rotated for more than 100 revolutions in an anticlockwise direction, and the rotary torque produced more than 40 pN nm^{-1} under high load. Soong *et al.* combined inorganic and biological materials in a hybrid system by fabricating nickel nanopropellers (length 750 to 1400 nm, diameter 150 nm) that were attached to the γδε-subunit of F_1-ATPase through

biotin–streptavidin linkages.[68] The torque on the motors were 20 and 19 pN nm^{-1} with a rotational velocity of 8.0 and 1.1 rps for the 750 and 1400 nm propeller, respectively. The F_1-ATPase motors were mounted on nickel-capped SiO_2 posts (height 200 nm) to prevent drag on the propellers due to proximity interactions with the substrate.

A reversible on/off 'switch' was added to the F_1-ATPase motor to control its function and the nanopropeller rotation. Liu *et al.* introduced a zinc-binding site to the αβ-subunit of the motor by site-directed mutagenesis. Rotation of the nanopropeller could then be inhibited in the presence of zinc because it interfered with the cyclic conformation changes that occurred during ATP hydrolysis. Removal of zinc by chelation restored both ATP hydrolysis and nanopropeller rotation.[69] Rondelez *et al.* was able to control the rotational direction of F_1 by attaching a magnetic bead to the γ-subunit and forcing F_1 to rotate clockwise against its chemical potential using magnetic tweezers.[70] When the magnetic field was removed, F_1 resumed its natural clockwise rotation through ATP hydrolysis. Single motors were captured in 6 fl microchambers to quantitatively measure the synthesis and accumulation of ATP by forced clockwise F_1 rotation.

Biological actuators with single cells or cell clusters

Unlike biomolecules, single cells and microorganisms can self-replicate and perform multiple functions at once, such as synthesizing organic and inorganic materials, sensing, communicating, converting energy, and generating mechanical motion. They are also larger in size and can be used to power microdevices in ways that would exceed the limits of conventional microfabrication technologies. Here, we discuss a number of cell-based biological actuators, including bacteria, protozoa, algae, and cardiomyocytes, and describe current efforts to control their movements externally.

Bacterial microorganisms

Several research groups have exploited the motility of bacteria for bioactuation because of the unique advantages of flagellar motors.[71] Many types of flagellar motors have already been well-studied.[72–75] Bacteria offers a degree of miniaturization of a fully-powered actuator that has not been achieved to date. Bacterial culture is also rapid and inexpensive, drawing chemical energy directly from the environment. Finally, they are controllable *en masse* through different sensory mechanisms and at wide ranges of temperatures and pH. However, the power and architecture of a single bacterium is limited – swarms are required to generate more thrust, and only certain monolayer geometries, such as spheres and cubes, have been used. Another important challenge is 3D motion control. Swarms are not centrally connected, and while they respond to some external stimuli, it is unclear how this stimuli will be used to generate 3D motion control, especially if the bacterium is tethered to the microstructure. Lastly, immune response must be addressed if the bacterial microorganisms are to be used in the body.

The flagellar motors can potentially be used as pumps to control fluid flow. Darnton *et al.* absorbed the cell bodies of *Serratia marcescens* swarmer cells onto flat polydimethylsiloxane (PDMS) surfaces to form bacterial "carpets" with freely rotating flagellar filaments.[76] Tracer beads (1 μm diameter) near the surface of the carpet were displaced, revealing linear and rotational flow patterns. They also made simple "automobile" chips and beads by similarly absorbing the swarmer cells to polystyrene beads (10 μm diameter) and various PDMS geometries to demonstrate translation and rotation. Kim *et al.* used these bacterial carpets in microfluidic channels to pump and mix two fluid streams.[77]

In addition, bacteria can be used to translate or rotate a microdevice. Hiratsuka *et al.* fabricated silicon dioxide micro-rotors and coated them with streptavidin.[78] The micro-rotors were released and attached to a silicon circular track functionalized with the sialic protein, fetuin. Biotinylated *Mycoplasma mobile* bacteria were introduced, binding to the micro-rotor and gliding unidirectionally along the track. As a result, rotation of the micro-rotor was achieved at a rate of 2 rpm. Similarly, Sokolov *et al.* harnessed the collective swimming of randomly moving *Bacillus subtilis* bacteria to directionally rotate asymmetric gears at 1–2 rpm.[79]

The transport of synthetic cargo can be achieved by selectively attaching the cell bodies of bacteria to it. Behkam *et al.* first proposed the method of patterning *Serratia marcescens* on polystyrene microbeads using reactive ion etching.[80] The patterned beads exhibited higher average velocities of 28.2 ± 10.5 μm s^{-1} compared to the velocities of unpatterned beads (14.8 ± 1.1 μm s^{-1}). Similarly, Cho *et al.* fabricated poly(ethylene glycol) (PEG) microbeads that were selectively-coated on one half of the microbeads with poly-L-lysine (PLL).[81] This was meant to enhance the velocity and directionality of the microbeads as opposed to coating the entire PEG microbead. *Salmonella typhimurium* bacteria were mixed with the PEG microbeads and allowed to attach selectively to PLL-coated regions. The microbeads traveled at an average velocity of 0.37 μm s^{-1}.

Finally, bacteria can be controlled externally to enhance desired functionalities. Sakar *et al.* controlled a monolayer of *Serratia marcescens* swarmer cells with galvanotaxis using direct current (DC) electric fields.[82] The swarmer cells were blotted on the surface of SU-8 rectangular microstructures (100 L × 50 W × 5 T) to form MicroBioRobots (MBRs). A star-shaped trajectory with 5 destination points was fed to a feedback control algorithm that used the real-time location of the MBR and the position of the next destination to control the applied voltage at a frequency of 8 Hz. Steager *et al.* used phototaxis as a switch to control a 50 μm triangular microstructure blotted with the swarmer cells.[83] After exposure of the cells with ultraviolet (UV) light, motility temporarily stopped until the light was removed. Finally, Martel *et al.* showed directional and velocity control of a magnetotactic bacterial strain, *Magnetospirillum marine coccus* (MC-1) using

a closed-loop computer system.[84] MC-1 swam in room-temperature water at max speeds around 300 μm s^{-1} and produced thrust forces exceeding 4 pN. This value is relatively high compared to other flagellated bacteria with a typical thrust force in the range of 0.3–0.5 pN.

Protozoan microorganisms

In parallel to the bacteria work, some research groups are using complex eukaryotic microorganisms for bioactuation. Itoh controlled the motion of *Paramecium caudatum*, a unicellular microorganism, by changing the electrical potential gradient of the culture medium.[85] The *Paramecium* exhibited negative galvanotaxis, and when a DC electric field was applied, the *Paramecium* aligned to the electric field and started to swim toward the cathode at an applied electric potential gradient of 0.3 V mm^{-1}. Using an automatic motion control program, the *Paramecium* was guided along a Fig. 8 and star-shaped course, and it was used to rotate a 1 mm micro-impeller. The maximum swimming speed of the *Paramecium* was above 2.0 mm s^{-1}, and the force generated was estimated to be about 27 nN. Guevorkian and Valles Jr. studied the *Paramecium* under a wide range of magnetic forces to determine the maximum propulsion force, or stall force, estimated to be 0.7 nN.[86]

Kim *et al.* used 'artificial' magnetotaxis to control the movement of *Tetrahymena pyriformis*, a ciliate protozoan, with ferromagnetic nanoparticles and an external time-varying magnetic field.[87] Spherical iron oxide particles (50 nm diameter) were internalized by the protozoa and magnetized. When an electromagnet with magnetic field strength of 2 mT was applied, the protozoa aligned (or anti-aligned depending on the dipole) to the field. A tracking algorithm was then used to guide a single protozoan through a sequence of five destination points.

Another ciliate protozoan, *Vorticella convallaria*, has a contractile stalk that is controllable by calcium concentration. In a microfluidic PDMS device, Nagai *et al.* injected cells into a chamber and cultured them for several hours until their stalks adhered to the glass surface.[88] The cells were permeabilized using saponin to control the contractile state of the stalk through external calcium concentration. An influx of in buffer containing either Ca^{2+} or Ca^{2+}-chelators resulted in contraction and relaxation, respectively. On average, contraction/relaxation states took under 2 seconds to complete, with the length of the stalks changing 40 μm between each state. Extracted *Vorticella convallaria* delivered high levels of force around 40 pN and a maximum contractile velocity of 8.8 cm s^{-1}.

Algal microorganisms

Weibel *et al.* took it a step further by attaching cargo loads to biflagellated algae, *Chlamydomonas reinhardtii*, steering the swimming cells to a targeted location with phototaxis, and releasing those loads with photochemistry (Fig. 2).[89] Specially-modified polystyrene beads (1 to 6 μm diameter) attached to the cells on contact. As long as the beads did not interfere with the flagella, the cells continued to travel at velocities between 100–200 μm s^{-1}. McCord *et al.* analyzed the force generation of *Chlamydomonas reinhardtii* using optical trapping and obtained a swimming force of 25.8 ± 8.3 pN for wild-type cells.[90] The loaded cells were placed in a microfluidic channel with low intensity LEDs (λ = 505 nm) embedded at both ends. Alternating LEDs were illuminated and the loaded cells swam back and forth with rapid phototactic responses (<1 s). The cells could be unloaded by photochemical cleavage of the modified polystyrene beads. UV irradiation (λ = 365 nm) of the cells released the loads within 18 seconds without damaging the cells.

Single and clustered cardiomyocytes

Cardiomyocytes are very promising as bioactuators because they are: (1) synchronous, (2) spontaneously contracting, and (3) powered by glucose as its only energy source without applied electrical power or stimulus.[91] A single cardiomyocyte can generate at least 1 μN of force. The concept of bioactuators using cultured cardiomyocytes is to couple them to polymer-based microstructures to convert chemical energy into mechanical energy to move the structures.

Tanaka *et al.* fabricated arrays of PDMS micropillars using a replica molding process and coated them with fibronectin to promote cardiomyocyte attachment.[92] Isolated from primary neonatal rat hearts, cardiomyocytes were cultured over the micropillars. About 80% of the pillars were coupled with cardiomyocytes that spontaneously beat at 1.4 Hz after the third day in culture. Contraction of the cardiomyocytes displaced the micropillars at a calculated force of 3.5 μN.

Park *et al.* fabricated arrays of PDMS microcantilevers using a sandwich molding process and coated them with a fibronectin–gelatin mixture.[93] Cardiomyocytes were seeded on the microcantilevers and contractile forces caused them to deflect. Using analytical and numerical analysis, the contractile force of the cardiomyocytes on the microcantilevers was 2–5 nN μm^{-2}. This was improved to 7–10 nN μm^{-2} by fabricating grooves on the microcantilevers. Thus, on their largest PDMS microcantilever with dimensions 150 × 750 μm, cardiomyocytes would be able to generate upwards of 1 mN peak forces.

Kim *et al.* developed a PDMS microgear using a sandwich molding process.[94] Poly(ethylene glycol) PEG microwells were patterned onto a glass substrate and the microwells were coated with collagen. The collagen selectively absorbed to the exposed glass. Small aggregates of cardiomyocytes were seeded on the microwells and had an estimated contractile force of 9.06 mN mm^{-2} (about 6 cells). A peak contractile force of 20 μN was measured. The PDMS microgears were gently attached to these cell aggregates. However, the authors did not show directional movement of the gears by contraction of the cardiomyocyte aggregates.

Biological actuators with natural and synthetic tissues

While biomolecules and unicellular microorganisms are being extensively studied as bioactuators, there is

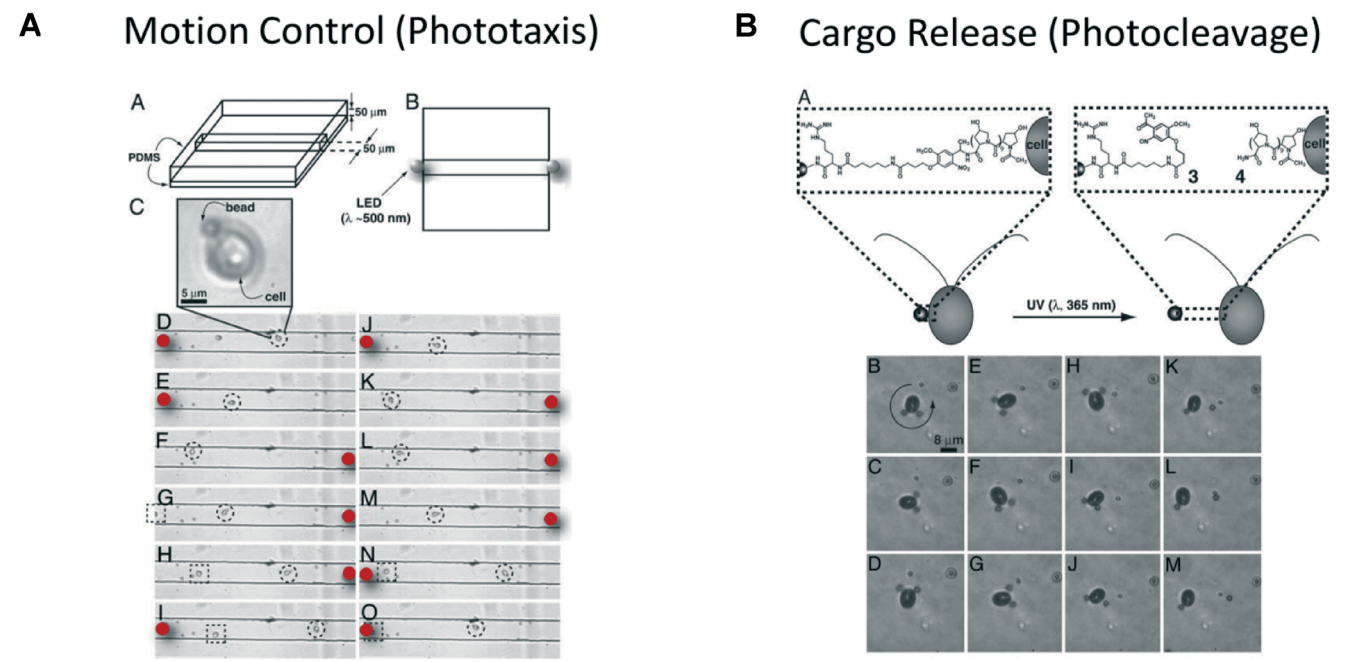

Fig. 2 Cellular-level biological machines. (A) Specially-modified polystyrene beads (1 to 6 μm diameter) were attached to biflagellated algae on contact. The cells were able to transport the beads at velocities of 100–200 μm s^{-1} and could be controlled through phototactic responses using low intensity LEDs (λ = 505 nm). (B) The cells could be unloaded by photochemical cleavage of the modified polystyrene beads. UV irradiation (λ = 365 nm) of the cells released the loads within 18 seconds without damaging the cells [reprinted from ref. 89].

surprisingly little effort directed towards the creation of bio-actuators with tissues and other complex hierarchies. Although single or small clusters of cells can drive micro-scale structures, it is difficult to do this for higher-ordered structures. Nature provides an elegant solution by forming complex hierarchies of tissues using cells as building blocks. This hierarchy of increasing complexity is tied to an increase in functionalities. Based on active and passive self-organization principles, it has been demonstrated that more complex hierarchical structures can work as bioactuators for improved functional performance. In this last section, we focus on research related to mammalian-derived cardiac- and skeletal-based tissues and also the early development of insect-derived dorsal vessel-based tissue as bioactuators.

Cardiac muscle-based tissues

The assembly of cell sheets of cardiomyocytes can be harnessed to generate larger forces and be used to drive more complicated structures or fluids. One method that garnered a lot of attention was the use of temperature-responsive polymers functionalized with cell-adhesive ligands to culture cell sheets of cardiomyocytes. Shimizu *et al.* uniformly grafted poly(*N*-isopropylacrylamide) (PIPAAm) on polystyrene culture dishes by irradiation with an electron beam.[95] PIPAAm is a thermo-responsive polymer that shows remarkable changes in swelling by changing its temperature. Above 32 °C, PIPAAm was compact and hydrophobic. Cells were able to adhere, grow, and form sheets on these surfaces. When the temperature was lowered, PIPAAm became hydrophilic and swollen. As a result, the cell sheets detached from the surface of the polymer (Fig. 3A). The cell attachment and adherence were prevented by the difficulty of displacing adsorbed water molecules on highly hydrated hydrophilic surfaces. The advantage of this technique was that only the connection between cell adhesive proteins and the PIPAAm surface was broken, and the cells remain connected together as a cell sheet. Cell sheets of cardiomyocytes grown using this method kept their cell–cell junctions, remained synchronous, and could be overlaid for increased contractility.[96] Contraction of 4 monolayers stacked on top of each other produced 1.18 ± 0.26 mN of force measured with a strain gauge.

While microdevices are usually powered by external energy sources, cell sheets of cardiomyocytes can be used to create self-actuated, wireless, and mechanochemical transducers that require no externally coupled energy source or stimuli. Tanaka *et al.* developed the first demonstration of a micropump powered by a cell sheet of cardiomyocytes.[97] A square microchip (2 × 2 cm) consisted of four PDMS-based elements: a push-bar, a chamber layer, a diaphragm membrane, and a microchannel layer with two holes for fluid transfer. A cell sheet of cardiomyocytes was layered on top of the push-bar and diaphragm. Spherical polystyrene tracking particles (1 μm diameter) were dispersed in the medium, and spontaneous, oscillating fluid motion was observed by their movement with optical microscopy. The fluid oscillating frequency was 0.7 Hz with 150 μm maximum linear displacement of tracking particles. Directional fluid flow was demonstrated with check valves, but only flow rates of 2 nL min^{-1} were achieved. The same group recently improved on their method by wrapping a sheet of functional primary

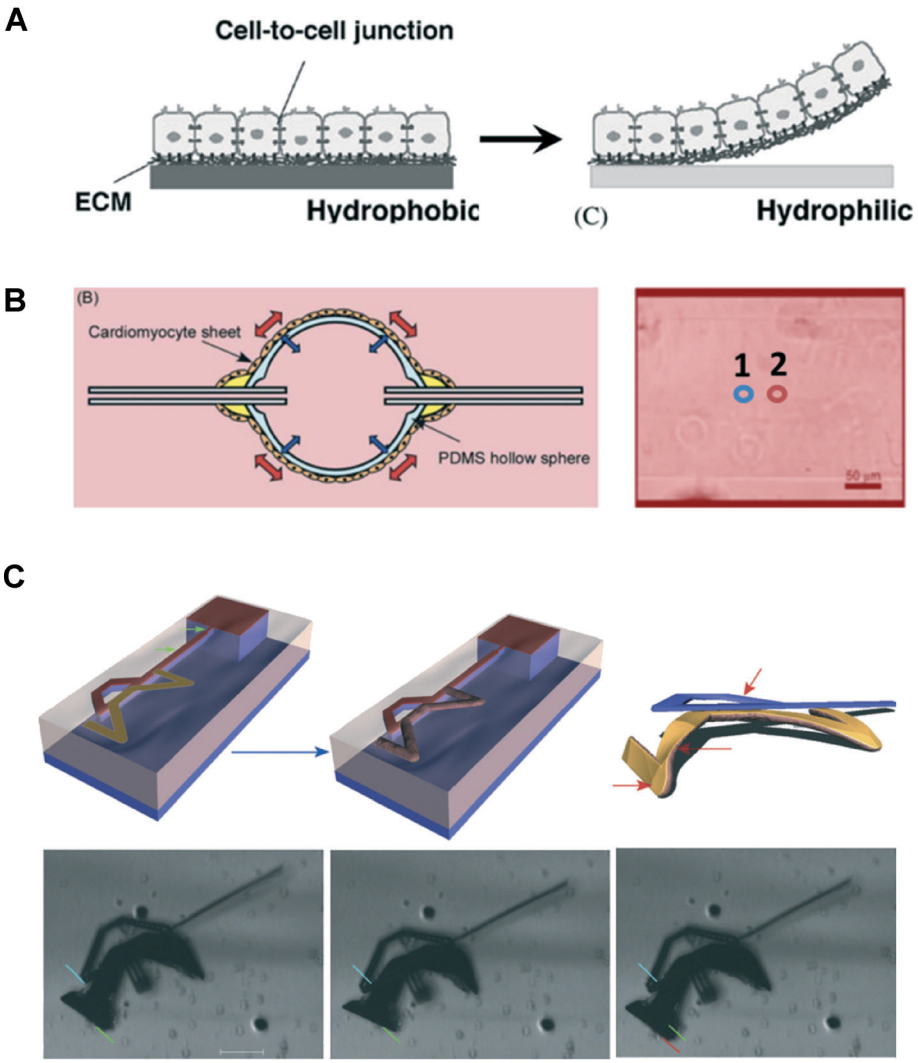

Fig. 3 Tissue-level biological machines. (A) Cardiomyocytes can be grown on thermo-responsive polymers called poly(*N*-isopropylacrylamide) (PIPAAm) to form a 2D cell sheet. These sheets can be detached intact by lowering the temperature below 32 °C [reprinted from ref. 95]. (B) The cell sheet of cardiomyocytes can be wrapped around a hollow PDMS sphere with inlet and outlet capillary tubes to engineer a bio-artificial hybrid pump. Oscillating fluid motion in the capillary was monitored by polystyrene tracking particles. The maximum observed linear displacement of tracking particles was 70 μm (1 to 2) [reprinted from ref. 98]. (C) Photolithographic techniques were used to fabricate a silicon microdevice with a chromium/gold layer. A sheet of cardiomyocytes was cultured on the beam and their contractions caused the beam to break from the rest of the device. This allowed the structure to "walk" freely [reprinted from ref. 99].

cardiomyocytes around a hollow PDMS sphere with inlet and outlet capillary tubes to engineer a bio-artificial hybrid pump (Fig. 3B).[98] The sphere is strained by the collective contractile motions of the attached cardiomyocyte sheet, and the fluid volume inside the hollow sphere chamber is reduced, producing flow into the capillary. The chamber diameter is millimeter-order (5 mm diameter); the capillaries are micrometer-order (200 μm inside diameter); the PDMS elastomer membrane is micrometer-order (250 μm thick). Oscillating fluid motion in the capillary was monitored by polystyrene tracking particles. The fluid oscillating frequency measured at 37 °C was 0.4 Hz and the maximum observed linear displacement of tracking particles was 70 μm. The expected flow rate was 47 nL min^{-1}, which was an improvement to the previous design.

Besides bioactuators that act like pumps to direct fluid flow, there has also been growing interest in creating structures that swim or walk with a sheet of cardiomyocytes. Xi *et al.* developed a microdevice using a silicon backbone with self-assembled cardiomyocytes grown on a chromium/gold layer.[99] They used photolithographic techniques to fabricate a micron-sized, self-assembled, and self-actuated walking bio-microactuator powered by cardiomyocyte muscular tissue. The muscle-bundle contraction force was reported to be 14 mN mm^2. Cardiomyocytes were aligned on a patterned film of Cr/Au, which was attached to a thin Si beam. After the microdevice was released from the PIPAAm coating, muscle contractions caused the beam to break from the rest of the device. This allowed the structure to "walk" freely (Fig. 3C). The leg dimensions were 138 μm long, 40 μm wide, and

20 nm/300 nm (Cr/Au) thick; the average step frequency was 1.8 Hz and its average maximum step size was 25 μm; the maximum speed was 38 μm s^{-1}. Kim *et al.* established a swimming microrobot by micromolding PDMS.[100] Using cardiomyocytes, cells were seeded on top of four conjoined cantilever beams that were grooved to influence the alignment and enhance their contractility relative to flat beams. An increase in force (88%) and bending (40%) was recorded, with an average swimming speed of 140 μm s^{-1}.

Feinberg *et al.* assembled cardiomyocytes on various PDMS thin films with proteins to create muscular thin films (MTFs).[101] When released from thermoresponsive polymers, the thin films curled or twisted into 3D conformations that purportedly performed gripping, pumping, walking (133 μm s^{-1}), and swimming functions (400 μm s^{-1}). The MTFs generated specific forces as high as 4 mN mm^{-2}. Recently, MTFs were used to reverse-engineer jellyfish-like constructs, dubbed "medusoids", by studying the structural design, stroke kinematics, and fluid–solid interactions of the *Aurelia aurita* moon jellyfish (Fig. 4A).[102] The artificial jellyfish, dubbed "medusoids", were composed of a bilayer of living muscle tissue and synthetic elastomer arranged in freely moveable lobes around a central disc. Medusoid propulsion, like that of jellyfish, was externally-driven by electrically-paced power and recovery strokes that alternately contracted the body into a quasi-closed "bell" and then relaxed into the open lobed form. Qualitative and quantitative comparisons of jellyfish and medusoid propulsion showed that the engineered system was able to replicate the momentum transport and body lengths traveled per swimming stroke of the natural system.

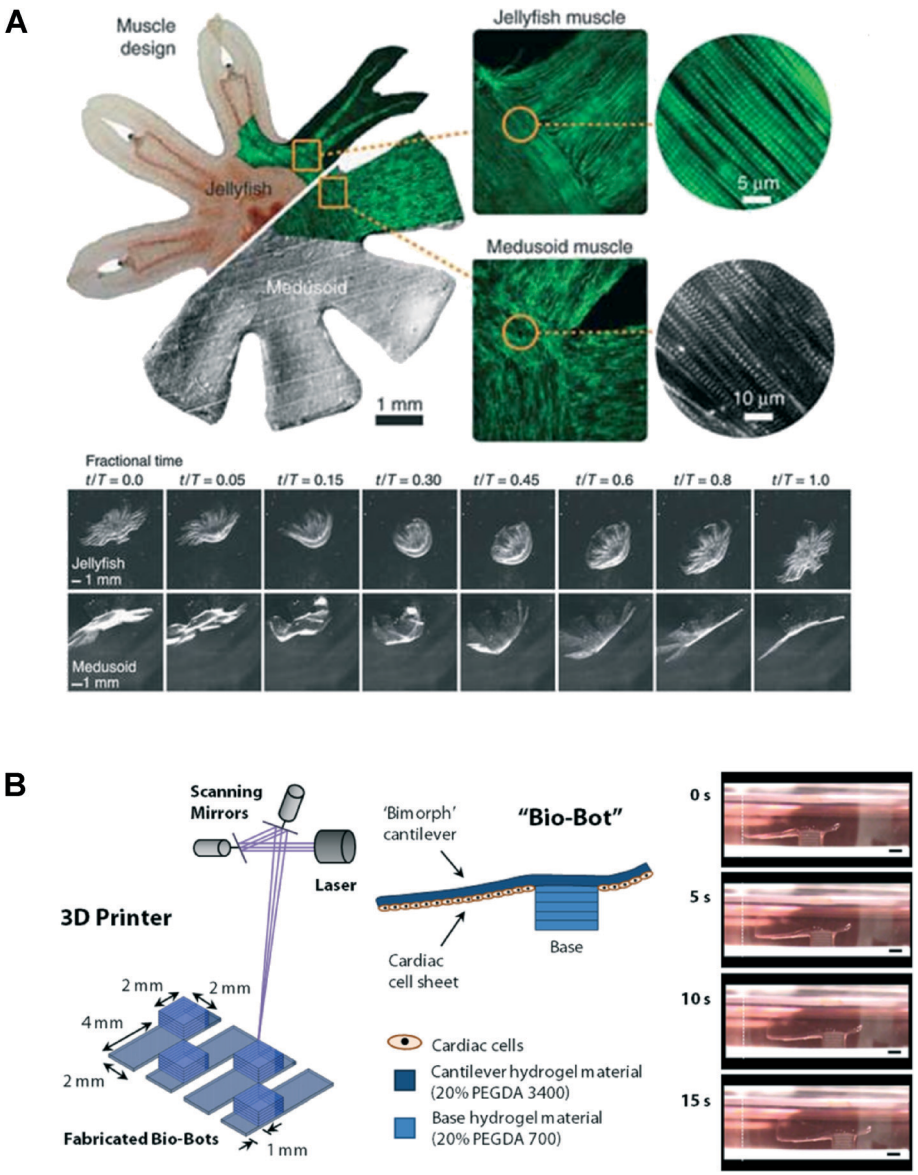

Fig. 4 Tissue-level biological machines. (A) A cell sheet of cardiomyocytes was grafted on PDMS thin films with carefully designed geometry and organized cells to mimic the swimming motion of jellyfish [reprinted from ref. 102]. (B) A walking "bio-bot" was constructed with a 3D printer by assembling layers of hydrogels and seeding cardiomyocytes on the backside of the 'bimorph' cantilever [reprinted from ref. 104].

Our group modified a 3D printer[103] for the assembly of "bio-bots"[104] with poly(ethylene glycol) (PEG) hydrogels and neonatal rat cardiomyocytes. The bio-bots consisted of a 'biological bimorph' cantilever structure as the actuator to power the bio-bot, and a base structure to define the asymmetric shape for locomotion. The cantilever structure was seeded with a sheet of contractile cardiac muscle cells on a variably-thick hydrogel layer. The thickness of the hydrogel layer and cytoskeletal tension from the cell sheet on the collagen-functionalized hydrogel determined the degree of curvature of the cantilever structure. When cardiomyocytes were seeded on the bio-bots, the contractile forces generated a power stroke that propelled the bio-bots forward (Fig. 4B). The physical (*i.e.* geometry and stiffness)[105] and chemical (*i.e.* growth factors and adhesive groups)[106] cues were spatially controlled with the 3D printer. The elastic properties of the bio-bots were tuned similar to that of neonatal rat cardiomyocytes to maximize their contractile force.[105] The maximum recorded velocity of the bio-bot was 236 μm s^{-1}, with an average displacement per power stroke of 354 μm and average beating frequency of 1.5 Hz.[104]

Skeletal muscle-based tissues

There is considerable interest in using skeletal muscle as a cell source for bio-bots and other cell-based bio-actuators because of the favorable attributes not available in cardiac muscle.[8] In the body, skeletal muscle facilitates movement by applying forces against bones and joints. The organization of the muscle is modular, having many longitudinally-aligned, multinucleated muscle fibers assembled together by connective tissue to form a densely-packed structure.[9] Recruitment of these fibers can be finely controlled by the nervous system, which innervates individual muscle fibers at localized regions.[7] By adjusting the number of contractile muscle fibers and the tension developed collectively, the nervous system can regulate graded muscle response for controlled movement.

To date, there are only a few published reports on the utilization of 2D skeletal muscle as bioactuators. The majority of applications investigated active tension of single or clusters of skeletal myotubes cultured on silicon,[107–110] collagen films,[111] and PDMS[112] cantilevers. In 3D, there are two current methods for engineering bioartificial skeletal muscle: (1) 2D-to-3D, and (2) 3D-to-3D. The first method was developed by Strohman *et al.*[113] and later refined by Dennis and Kosnik.[114,115] It consisted of myotubes, fibroblasts, cell-secreted ECM, and synthetic tendons. The beauty of this approach was that it did not require a pre-existing scaffold. Briefly, PDMS was set in a culture dish, and absorbed with a thin layer of laminin. Synthetic tendons were fixed at opposite ends and at a desired distance apart. Cells of myoblasts and fibroblasts were seeded, and upon reaching confluence, the medium was switched from growth to differentiation. After 2–3 weeks, the monolayer of myotubes would detach and self-organize to form a 3D muscle strip, dubbed 'myooids'. Huang *et al.* later modified the method to improve the speed of myooid formation.[116] Lam *et al.* used wavy PDMS substrates to align the myotubes in the myooids.[117] The second method was developed by Vandenburgh *et al.*,[118] although many variations exist.[119–121] It typically consisted of a pre-existing scaffold in 3D, either derived naturally (most common) or synthetically. Myoblasts with or without fibroblasts were embedded in the 3D scaffold and casted in molds. The molds were there for 3D scaffolds compacted by cells to retain certain shapes, such as strips[122] and rings.[123] Vandenburgh *et al.* formed skeletal muscle strips by microposts to measure maximum tetanic force of about 45 μN after 7–12 days of differentiation.[124] Fujita *et al.* formed skeletal muscle rings by magnetite-incorporation in skeletal myoblasts to produce about 1 μN of force when electrically-stimulated after 5–8 days of differentiation.[125] Yamamoto *et al.* later used this same technique with microposts to record 33.2 μN of twitch force.[126] Herr and Dennis demonstrated a swimming robot actuated by living skeletal muscle (Fig. 5A).[127] It was actuated by two explanted frog semitendinosus muscles and controlled by an embedded microcontroller with muscle stimulators. Using open loop stimulation protocols, the robot performed basic swimming maneuvers such as starting, stopping, turning (400 mm radius), and straight-line swimming (>1/3 body lengths per second). The robot swam for a total of 4 hour over a 42 hour lifespan before its velocity degraded below 75% of its max. The length of the robot is nearly 80 cm long.

Consequently, skeletal muscle can be used in bio-bots and other bio-actuator designs to reversibly switch locomotion on/off by neural signals, to regulate displacement and pacing by altering the combined contractile force, and to generate a wide range of motion by localized innervation of muscle fibers. Optical methods have been developed to depolarize or hyperpolarize neurons using specific wavelengths of light.[128–130] This method, known as 'optogenetics,' combines the temporal and spatial precision of light pulses with cellular specificity of genetic targeting. The general strategy of optogenetics involves introducing a light-sensitive protein, such as channelrhodopsin-2 (ChR2, discovered in green algae) to a specific cell type, illuminating the cells with defined spatio-temporal parameters, and obtaining reliable readout of the cellular behavior.[131] This past year, the method was applied to cardiac[132,133] and skeletal[134,135] muscle cells to rhythmically control their contractions. It was also used to locally innervate specific regions of muscle tissue to generate movement in multiple degrees of freedom (multi-DOF). Overall, the advantage of optogenetics is its fast, precise, and local stimulation of cells and tissues, relative to electrical stimulation.

Furthermore, several research groups are developing methods to direct heterotypic cell–cell interactions between neurons and muscle cells, which can be used to regulate muscle contraction through neuromuscular junctions.[136–139] Neurons can drive the synthesis of neurotransmitters that initiate action potentials and activate muscle contraction. More recently, Kabumoto *et al.* developed a prosthetic-like

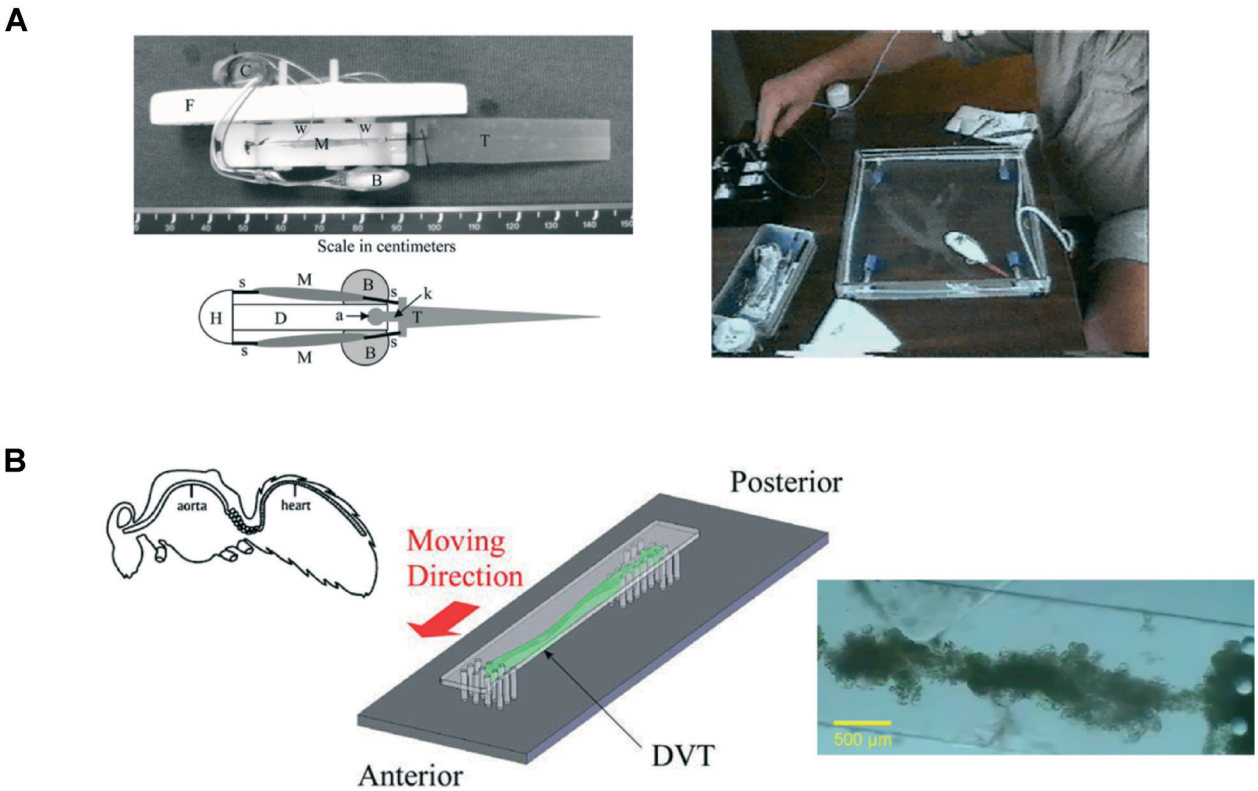

Fig. 5 Tissue-level biological machines. (A) Two explanted frog semitendinosus muscles (M) were attached by sutures (s) to a swimming robot for actuation. The robot was controlled by an embedded microcontroller with muscle stimulators. Basic swimming maneuvers such as starting, stopping, turning (400 mm radius), and straight-line swimming (>1/3 body lengths per second) were demonstrated [reprinted from ref. 127]. (B) The muscular power from dorsal vessel tissues (DVTs) of insects can also be used as actuators and are robust between 5–40 °C. DVTs from the larvae of lepidopteran inchworms (*Ctenoplusia agnate*) were fixed between micropillars of a "polypod microrobot" (PMR) made out of micromolded PDMS, which moved at 3.5 ± 0.7 μm s^{-1} with a contractile force of 20 μN. Electrical stimulation could be applied at 10 V with 20 ms durations and 50 ms delays to regulate contractility and force output [reprinted from ref. 142].

microdevice with living skeletal tissue.[140] The microdevice was molded from PDMS in the shape of a 'micro-hand' gripper, and the 3D-to-3D skeletal tissue was anchored to two pillars on the gripper. Surface electromyogram signals from a subject's hand movement generated electric pulses into the culture medium of the gripper that triggered skeletal tissue contraction. The displacement between the two pillars was only on the order of a few micrometers, but the overall demonstration of skeletal tissue control was promising. Functional performance should continue to improve as new advances in skeletal muscle tissue engineering emerge.

Insect dorsal vessel-based tissues

Research groups are also beginning to take advantage of the muscular power from the dorsal vessels of insects to power actuators because of their robustness between 5 and 40 °C. The dorsal vessel of insects is the major structural component of an insect's circulatory system. It is a tube that runs longitudinally through the thorax and abdomen, along the inside of the dorsal body wall. In the abdomen, the dorsal vessel is called the heart, and it has valves and musculature that contract autonomously. Akiyama *et al.* removed the dorsal vessel tissue (DVT) from the larvae of lepidopteran inchworms (*Ctenoplusia agnate*) and fixed them between micropillars of a "polypod microrobot" (PMR) made out of micromolded PDMS (12.5 L × 1.35 W × 0.2 T mm dimensions) (Fig. 5B).[141] The PMR moved at 3.5 ± 0.7 μm s^{-1} with a contractile force of 20 μN. Electrical stimulation could be applied at 10 V with 20 ms durations and 50 ms delays to regulate contractility and force output. In a separate study, dorsal vessel tissue of *Drosophila melanogaster* larvae were also excised and demonstrated to contract on their micropillars at 1.6 Hz with a contractile force of 197 nN.[142]

Conclusion

This review highlights the recent advancements in the emerging field of bioactuators across a multitude of length scales, including biomolecules, cells and microorganisms, and tissues. Clearly, there is an emphasis on closing the feedback loop between the biological and engineering worlds, and to use biological systems to improve engineering ones. However, despite the significant progress in the last few years, there are still plenty of opportunities to explore and challenges to overcome. In addition, this review is limited to one

functional element, that of actuation. There are a number of other elements to be developed, such as sensing, information processing, protein expression, and transport. It is the realization and utility of all of these functional elements, either alone or combined, that will have significant impact in health, security, and the environment. These bioactuators represent one key component in this grand vision, and future developments will depend on an integrated approach to combine them in an effort to perform prescribed tasks.

Acknowledgements

We would like to acknowledge our funding from the National Science Foundation (NSF), Science and Technology Center (STC), and Emergent Behaviors in Integrated Cellular Systems (EBICS) grant CBET-0939511.

References

1 T. McMahon and J. T. Bonner, *On size and life*, Scientific American, 1983.
2 M. Piccolino, Biological machines: from mills to molecules, *Nat. Rev. Mol. Cell Biol.*, 2000, **1**, 149–152.
3 L. Sherwood, *Human physiology: from cells to systems*, Brooks Cole, 2012.
4 X. Xiong, M. E. Lidstrom and B. A. Parviz, Microorganisms for MEMS, *J. Microelectromech. Syst.*, 2007, **16**, 429–444.
5 R. D. Kamm, R. Nerem and K. J. Hsia, Cells into systems, *Mechanical Engineering Magazine*, 2010.
6 A. M. King, D. S. Loiselle and P. Kohl, Force generation for locomotion of vertebrates: skeletal muscle overview, *IEEE J. Oceanic Eng.*, 2004, **29**, 684–691.
7 R. D. Kamm and R. Bashir, Creating living cellular machines, *Ann. Biomed. Eng.*, DOI: 10.1007/s10439-013-0902-7.
8 B. J. Nelson, I. K. Kaliakatsos and J. J. Abbott, Microrobots for minimally invasive medicine, *Annu. Rev. Biomed. Eng.*, 2010, **12**, 55–85.
9 M. Knoblauch and W. S. Peters, Biomimetic actuators: where technology and cell biology merge, *Cell. Mol. Life Sci.*, 2004, **61**, 2497–2509.
10 A. M. R. Kabir, A. Kakugo, J. P. Gong and Y. Osada, How to integrate biological motors towards bio-actuators fueled by ATP, *Macromol. Biosci.*, 2011, **11**, 1314–1324.
11 N. C. Seeman, *et al.*, New motifs in DNA nanotechnology, *Nanotechnology*, 1998, **9**, 257–273.
12 P. W. K. Rothemund, Folding DNA to create nanoscale shapes and patterns, *Nature*, 2006, **440**, 297–302.
13 C. Mao, W. Sun, Z. Shen and N. C. Seeman, A nanomechanical device based on the B–Z transition of DNA, *Nature*, 1999, **397**, 144–146.
14 B. Yurke, A. J. Turberfield, A. P. Mills, F. C. Simmel and J. L. Neumann, A DNA-fuelled molecular machine made of DNA, *Nature*, 2000, **406**, 605–608.
15 C. Bustamante, Z. Bryant and S. B. Smith, Ten years of tension: single-molecule DNA mechanics, *Nature*, 2003, **421**, 423–427.
16 F. C. Simmel and B. Yurke, Using DNA to construct and power a nanoactuator, *Phys. Rev. E: Stat., Nonlinear, Soft Matter Phys.*, 2001, **63**, 041913.
17 J.-S. Shin and N. A. Pierce, A synthetic DNA walker for molecular transport, *J. Am. Chem. Soc.*, 2004, **126**, 10834–10835.
18 T. Omabegho, R. Sha and N. C. Seeman, A bipedal DNA Brownian motion with coordinated legs, *Science*, 2009, **324**, 67–71.
19 Y. Tian and C. Mao, Molecular gears: a pair of DNA circles continuously rolls against each other, *J. Am. Chem. Soc.*, 2004, **126**, 11410–11411.
20 P. Yin, H. Yan, X. G. Daniel, A. J. Turberfield and J. H. Reif, A unidirectional DNA walker that moves autonomously along a track, *Angew. Chem., Int. Ed.*, 2004, **43**, 4906–4911.
21 Y. Tian, Y. He, Y. Chen, P. Yin and C. Mao, A DNAzyme that walks processively and autonomously along a one-dimensional track, *Angew. Chem., Int. Ed.*, 2005, **44**, 4355–4358.
22 R. Pei, S. K. Taylor, D. Stefanovic, S. Rudchenko, T. E. Mitchell and M. N. Stojanovic, Behavior of polycatalytic assemblies in a substrate-displaying matrix, *J. Am. Chem. Soc.*, 2006, **128**, 12693.
23 K. Lund, *et al.*, Molecular robots guided by prescriptive landscapes, *Nature*, 2010, **465**, 206–210.
24 R. A. Muscat, J. Bath and A. J. Turberfield, A programmable molecular robot, *Nano Lett.*, 2011, **11**, 982–987.
25 E. Nogales, Structural insights into microtubule function, *Annu. Rev. Biochem.*, 2000, **69**, 277–302.
26 R. Vale, T. Reese and M. Sheetz, Identification of a novel force-generating protein, kinesin, involved in microtubule-based motility, *Cell*, 1985, **42**, 39–50.
27 N. Hirokawa, Y. Noda, Y. Tanaka and S. Niwa, Kinesin superfamily motor proteins and intracellular transport, *Nat. Rev. Mol. Cell Biol.*, 2009, **10**, 682–696.
28 D. C. Turner, C. Chang, K. Fang, S. L. Brandow and D. B. Murphy, Selective adhesion of functional microtubules to patterned silane surfaces, *Biophys. J.*, 1995, **69**, 2782–2789.
29 D. Turner, C. Chang, K. Fang, P. Cuomo and D. Murphy, Kinesin movement on glutaraldehyde-fixed microtubules, *Anal. Biochem.*, 1996, **242**, 20–25.
30 L. Limberis, J. Magda and R. Stewart, Polarized alignment and surface immobilization of microtubules for kinesin-powered nanodevices, *Nano Lett.*, 2001, **1**, 277–280.
31 R. Doot, H. Hess and V. Vogel, Engineered networks of oriented microtubule filaments for directed cargo transport, *Soft Matter*, 2007, **3**, 349–356.
32 G. Muthukrishnan, B. M. Hutchins, M. E. Williams and W. O. Hancock, Transport of semiconductor nanocrystals by kinesin molecular motors, *Small*, 2006, **2**, 626–630.
33 C. Bottier, *et al.*, Active transport of oil droplets along oriented microtubules by kinesin molecular motors, *Lab Chip*, 2009, **9**, 1694–1700.
34 R. Yokokawa, *et al.*, Hybrid nanotransport system by biomolecular linear motors, *J. Microelectromech. Syst.*, 2004, **13**, 612–619.

35 R. Yokokawa, M. C. Tarhan, T. Kon and H. Fujita, Simultaneous and bidirectional transport of kinesin-coated microspheres and dynein-coated microspheres on polarity-oriented microtubules, *Biotechnol. Bioeng.*, 2008, **101**, 1–8.

36 J. Howard, A. J. Hudspeth and R. D. Vale, Movement of microtubules by single kinesin molecules, *Nature*, 1989, **342**, 154–158.

37 Y. Hiratsuka, T. Tada, K. Oiwa, T. Kanayama and T. Q. P. Uyeda, Controlling the direction of kinesin-driven microtubule movements along microlithographic tracks, *Biophys. J.*, 2001, **81**, 1555–1561.

38 H. Hess, J. Clemmens, C. M. Matzke, G. D. Bachand, B. C. Bunker and V. Vogel, Ratchet patterns sort molecular shuttles, *Appl. Phys. A: Mater. Sci. Process.*, 2002, **75**, 309–313.

39 J. Clemmens, *et al.*, Motor-protein 'roundabouts': microtubules moving on kinesin-coated tracks through engineered networks, *Lab Chip*, 2004, **4**, 83.

40 R. Yokokawa, Y. Yoshida, S. Takeuchi, T. Kon and H. Fujita, Unidirectional transport of a bead on a single microtubule immobilized in a submicrometre channel, *Nanotechnology*, 2006, **17**, 289–294.

41 C. Lin, M. Kao, K. Kurabayashi and E. Meyhofer, Efficient designs for powering microscale devices with nanoscale biomolecular motors, *Small*, 2006, **2**, 281–287.

42 H. Hess, *et al.*, Molecular shuttles operating undercover: a new photolithographic approach for the fabrication of structured surfaces supporting directed motility, *Nano Lett.*, 2003, **3**, 1651–1655.

43 R. Yokokawa, Y. Yoshida, S. Takeuchi, T. Kon and H. Fujita, Unidirectional transport of kinesin-coated beads on microtubules oriented in a microfluidic device, *Nano Lett.*, 2004, **11**, 2265–2270.

44 M. van den Heuvel, M. de Graaff and C. Dekker, Molecular sorting by electrical steering of microtubules in kinesin-coated channels, *Science*, 2006, **312**, 910–914; B. M. Hutchins, M. Platt, W. O. Hancock and M. E. Williams, Directing transport of $CoFe_2O_4$-functionalized microtubules with magnetic fields, *Small*, 2007, **3**, 126–131.

45 A. K. Boal, G. D. Bachand, S. B. Rivera and B. C. Bunker, Interactions between cargo-carrying biomolecular shuttles, *Nanotechnology*, 2006, **17**, 349–354.

46 C. Brunner, C. Wahnes and V. Vogel, Cargo pick-up from engineered loading stations by kinesin driven molecular shuttles, *Lab Chip*, 2007, **7**, 1263–1271.

47 G. D. Bachand, S. B. Rivera, A. K. Boal, J. Gaudioso, J. Liu and B. C. Bunker, Assembly and transport of nanocrystal CdSe quantum dot nanocomposites using microtubules and kinesin motor proteins, *Nano Lett.*, 2004, **4**, 817–821.

48 S. Diez, *et al.*, Stretching and transporting DNA molecules using motor proteins, *Nano Lett.*, 2003, **3**, 1251–1254.

49 C. Z. Dinu, *et al.*, Parallel manipulation of bifunctional DNA molecules on structured surfaces using kinesin-driven microtubules, *Small*, 2006, **2**, 1090–1098.

50 G. D. Bachand, S. B. Rivera, A. Carroll-Portillo, H. Hess and M. Bachand, Active capture and transport of virus particles using a biomolecular motor-driven, nanoscale antibody sandwich assay, *Small*, 2006, **2**, 381–385.

51 B. D. Martin, *et al.*, An engineered virus as a bright fluorescent tag and scaffold for cargo proteins – capture and transport by gliding microtubules, *J. Nanosci. Nanotechnol.*, 2006, **6**, 2451–2460.

52 M. Tarhan, R. Yokokawa, C. Bottier, D. Collard and H. Fujita, A nano-needle/microtubule composite gliding on a kinesin-coated surface for target molecule transport, *Lab Chip*, 2010, **10**, 86–91.

53 S. Hiyama, *et al.*, Autonomous loading, transport, and unloading of specific cargoes by using DNA hybridization and biological motor-based motility, *Small*, 2008, **4**, 410–415.

54 S. Hiyama, R. Gojo, T. Shima, S. Takeuchi and K. Sutoh, Biomolecular-motor-based nano- or microscale particle translocation on DNA microarrays, *Nano Lett.*, 2009, **9**, 2407–2413.

55 C. Schmidt and V. Vogel, Molecular shuttles powered by motor proteins: loading and unloading stations for nanocargo integrated into one device, *Lab Chip*, 2010, **10**, 2195–2198.

56 A. Carroll-Portillo, M. Bachand, A. C. Greene and G. D. Bachand, In vitro capture, transport, and detection of protein analytes using kinesin-based nanoharvesters, *Small*, 2009, **5**, 1835–1840.

57 K. Fujimoto, M. Kitamura, M. Yokokawa, I. Kanno, H. Kotera and R. Yokokawa, Colocalization of quantum dots by reactive molecules carried by motor proteins on polarized microtubule arrays, *ACS Nano*, 2013, **7**, 447–455.

58 D. Bray, *Cell movements: from molecules to motility*, Garland Science, 2000.

59 W. H. Guilford, *et al.*, Smooth muscle and skeletal muscle myosins produce similar unitary forces and displacements in the laser trap, *Biophys. J.*, 1997, **72**, 1006–1021.

60 J. A. Spudich, The myosin swinging cross-bridge model, *Nat. Rev. Mol. Cell Biol.*, 2001, **2**, 387–392.

61 A. F. Huxley, Mechanics and models of the myosin motor, *Philos. Trans. R. Soc., B*, 2000, **355**, 433–440.

62 R. D. Vale and R. A. Milligan, The way things move: looking under the hood of molecular motor proteins, *Science*, 2000, **288**, 88–95.

63 M. J. Tyska and M. S. Mooseker, Myosin-V motility: these levers were made for walking, *Trends Cell Biol.*, 2003, **13**, 447–451.

64 P. Pierobon, *et al.*, Velocity, processivity, and individual steps of single myosin V molecules in live cells, *Biophys. J.*, 2009, **96**, 4268–4275.

65 A. D. Mehta, *et al.*, Myosin-V is a processive actin-based motor, *Nature*, 1999, **400**, 590–593.

66 F. Gittes, B. Mickey, J. Nettleton and J. Howard, Flexural rigidity of microtubulesand actin filaments measured from thermal fluctuations in shape, *J. Cell Biol.*, 1993, **120**, 923–934.

67 H. Noji, R. Yasuda, M. Yoshida and K. Kinosita, Direct observation of the rotation of F1-ATPase, *Nature*, 1997, **386**, 299–302.

68 R. K. Soong, *et al.*, Powering an inorganic nanodevice with a biomolecular motor, *Science*, 2000, **290**, 1555–1558.

69 H. Liu, *et al.*, Control of a biomolecular motor-powered nanodevice with an engineered chemical switch, *Nat. Mater.*, 2002, **1**, 173–177.

70 Y. Rondelez, *et al.*, Highly coupled ATP synthesis by F_1-ATPase single molecules, *Nature*, 2005, **433**, 773–777.

71 E. B. Steager, *et al.*, Bacteria-powered microrobots, *Microbiorobotics*, 2012, ch. 10, pp. 249–275.

72 G. E. Murphy, J. R. Leadbetter and G. J. Jensen, In situ structure of the complete Treponema primitia flagellar motor, *Nature*, 2006, **442**, 1062–1064.

73 H. C. Berg and L. Turner, Torque generated by the flagellar motor of Escherichia coli, *Biophys. J.*, 1993, **85**, 2201–2216.

74 Y. Magariyama, *et al.*, Very fast flagellar rotation, *Nature*, 1994, **371**, 752.

75 Y. Magariyama, *et al.*, Simultaneous measurement of bacterial flagellar rotation rate and swimming speed, *Biophys. J.*, 1995, **69**, 2154–2162.

76 N. Darnton, L. Turner, K. Breuer and H. C. Berg, Moving fluid with bacterial carpets, *Biophys. J.*, 2004, **86**, 1863–1870.

77 M. J. Kim and K. S. Breuer, Use of bacterial carpets to enhance mixing in microfluidic systems, *J. Fluids Eng.*, 2007, **129**, 319–324.

78 Y. Hiratsuka, M. Miyata, T. Tada and T. Q. P. Uyeda, A microrotary motor powered by bacteria, *Proc. Natl. Acad. Sci. U. S. A.*, 2006, **103**, 13618–13623.

79 A. Sokolov, M. M. Apodaca, B. A. Grzybowski and I. S. Aranson, Swimming bacteria power microscopic gears, *Proc. Natl. Acad. Sci. U. S. A.*, 2010, **107**, 969–974.

80 B. Behkam and M. Sitti, Effect of quantity and configuration of attached bacteria on bacterial propulsion of microbeads, *Appl. Phys. Lett.*, 2008, **93**, 223901.

81 S. Cho, S. J. Park, S. Y. Ko, J.-O. Park and S. Park, Development of bacteria-based microrobot using biocompatible poly(ethylene glycol), *Biomed. Microdevices*, 2012, **14**, 1019–1025.

82 M. S. Sakar, *et al.*, Modeling, control and experimental characterization of microbiorobots, *Int. J. Robot. Res.*, 2011, **30**, 647–658.

83 E. Steager, *et al.*, Control of microfabricated structures powered by flagellated bacteria using phototaxis, *Appl. Phys. Lett.*, 2007, **90**, 263901.

84 S. Martel, M. Mohammadi, O. Felfoul, Z. Lu and P. Pouponneau, Flagellated magnetotactic bacteria as controlled MRI-trackable propulsion and steering systems for medical nanorobots operating in the human microvasculature, *Int. J. Robot. Res.*, 2009, **28**, 571–582.

85 A. Itoh, Motion control of protozoa for bio MEMS, *IEEE/ASME International Conference on Advanced Intelligent Mechatronics*, 1999, pp. 27–32.

86 K. Guevorkian and J. M. Valles Jr., Swimming Paramecium in magnetically stimulated enhanced, reduced, and inverted gravity environments, *Proc. Natl. Acad. Sci. U. S. A.*, 2006, **103**, 13051–13056.

87 D. H. Kim, U. K. Cheang, L. Kőhidai, D. Byun and M. J. Kim, Artificial magnetotactic motion control of Tetrahymena pyriformis using ferromagnetic nanoparticles: a tool for fabrication of microbiorobots, *Appl. Phys. Lett.*, 2010, **97**, 173702.

88 M. Nagai, S. Ryu, T. Thorsen, P. Matsudaira and H. Fujita, Chemical control of Vorticella bioactuator using microfluidics, *Lab Chip*, 2010, **10**, 1574–1578.

89 D. B. Weibel, *et al.*, Microoxen: microorganisms to move microscale loads, *Proc. Natl. Acad. Sci. U. S. A.*, 2005, **102**, 11963–11967.

90 R. P. McCord, J. N. Yukich and K. K. Bernd, Analysis of force generation during flagellar assembly through optical trapping of free-swimming Chlamydomonas reinhardtii, *Cell Motil. Cytoskeleton*, 2005, **61**, 137–144.

91 Y. Tanaka, *et al.*, Biological cells on microchips: New technologies and applications, *Biosens. Bioelectron.*, 2007, **23**, 449–458.

92 Y. Tanaka, *et al.*, Demonstration of a PDMS-based bio-microactuator using cultured cardiomyocytes to drive polymer micropillars, *Lab Chip*, 2006, **6**, 230–235.

93 J. Park, *et al.*, Real-time measurement of the contractile forces of self-organized cardiomyocytes on hybrid biopolymer microcantilevers, *Anal. Chem.*, 2005, **77**, 6571–6580.

94 D. H. Kim, *et al.*, Fabrication of patterned micromuscles with high activity for powering biohybrid microdevices, *Sens. Actuators, B*, 2006, **117**, 391–400.

95 T. Shimizu, M. Yamato, A. Kikuchi and T. Okano, Cell sheet engineering for myocardial tissue reconstruction, *Biomaterials*, 2003, **24**, 2309–2316.

96 T. Shimizu, *et al.*, Fabrication of pulsatile cardiac tissue grafts using a novel 3-dimensional cell sheet manipulation technique and temperature-responsive cell culture surfaces, *Circ. Res.*, 2002, **90**, e40–e48.

97 Y. Tanaka, *et al.*, An actuated pump on-chip powered by cultured cardiomyocytes, *Lab Chip*, 2006, **6**, 362–368.

98 Y. Tanaka, *et al.*, A micro-spherical heart pump powered by cultured cardiomyocytes, *Lab Chip*, 2007, **7**, 207–212.

99 J. Xi, J. J. Schmidt and C. D. Montemagno, Self-assembled microdevices driven by muscle, *Nat. Mater.*, 2005, **4**, 180–184.

100 J. Kim, *et al.*, Establishment of a fabrication method for a long-term actuated hybrid cell robot, *Lab Chip*, 2007, **7**, 1504–1508.

101 A. W. Feinberg, *et al.*, Muscular thin films for building actuators and powering devices, *Science*, 2007, **317**, 1366–1370.

102 J. C. Nawroth, *et al.*, A tissue-engineered jellyfish with biomimetic propulsion, *Nat. Biotechnol.*, 2012, **30**, 792–797.

103 V. Chan, P. Zorlutuna, J. H. Jeong, H. Kong and R. Bashir, Three-dimensional photopatterning of hydrogels using stereolithography for long-term cell encapsulation, *Lab Chip*, 2010, **10**, 2062–2070.

104 V. Chan, K. Park, M. B. Collens, H. Kong, T. A. Saif and R. Bashir, Development of miniaturized walking biological machines, *Sci. Rep.*, 2012, **2**, 857.

105 V. Chan, J. H. Jeong, P. Bajaj, M. B. Collens, H. Kong and R. Bashir, Multi-material bio-fabrication of hydrogel

cantilevers and actuators with stereolithography, *Lab Chip*, 2012, **12**, 88–98.
106 V. Chan, M. B. Collens, K. Park, J. H. Jeong, H. Kong and R. Bashir, Directed cell growth and alignment on protein-patterned 3D hydrogels with stereolithography, *Virtual Phys. Prototyp.*, 2012, **7**, 219–228.
107 K. Wilson, M. Das, K. J. Wahl, R. J. Colton and J. J. Hickman, Measurement of contractile stress generated by cultured rat muscle on silicon cantilevers for toxin detection and muscle performance enhancement, *PLoS One*, 2010, **5**, e11042.
108 M. Das, K. Wilson, P. Molnar and J. J. Hickman, Differentiation of skeletal muscle and integration of myotubes with silicon microstructures using serum-free medium and a synthetic silane substrate, *Nat. Protoc.*, 2007, **2**, 1795–1801.
109 K. Shimizu, H. Fujita and E. Nagamori, Micropatterning of single myotubes on a thermoresponsive culture surface using elastic stencil membranes for single-cell analysis, *J. Biosci. Bioeng.*, 2010, **109**, 174–178.
110 H. Fujita, T. D. Van, K. Shimizu, R. Hatsuda, S. Sugiyama and E. Nagamori, Designing of a Si-MEMS device with an integrated skeletal muscle cell-based bio-actuator, *Biomed. Microdevices*, 2011, **13**, 123–129.
111 H. Fujita, K. Shimizu and E. Nagamori, Novel method for measuring active tension generation by C2C12 myotube using UV-crosslinked collagen film, *Biotechnol. Bioeng.*, 2010, **106**, 482–489.
112 Y. Sun, R. Duffy, A. Lee and A. W. Feinberg, Optimizing the structure and contractility of engineered skeletal muscle thin films, *Acta Biomater.*, 2013, **9**, 7885–7894.
113 R. C. Strohman, E. Bayne, D. Spector, T. Obinata, J. Micou-Eastwood and A. Maniotis, Myogenesis and histogenesis of skeletal muscle on flexible membranes in vitro, *In Vitro Cell. Dev. Biol.*, 1990, **26**, 210–208.
114 R. G. Dennis and P. E. Kosnik, Excitability and isometric contractile properties of mammalian skeletal muscle constructs engineered in vitro, *In Vitro Cell. Dev. Biol.: Anim.*, 2000, **36**, 327–335.
115 R. G. Dennis, P. E. Kosnik, M. E. Gilbert and J. A. Faulkner, Excitability and contractility of skeletal muscle engineered from primary cultures and cell lines, *Am. J. Physiol.*, 2001, **280**, 288–295.
116 Y. C. Huang, R. G. Dennis and K. Baar, Cultured slow vs. fast skeletal muscle cells differ in physiology and responsiveness to stimulation, *Am. J. Physiol.*, 2006, **291**, C11–17.
117 M. T. Lam, Y. C. Huang, R. K. Birla and S. Takayama, Microfeature guided skeletal muscle tissue engineering for highly organized 3-dimensional free-standing constructs, *Biomaterials*, 2009, **30**, 1150–1155.
118 H. Vandenburgh, S. Swasdison and P. Karlisch, Computer-aided mechanogenesis of skeletal muscle organs from single cells in vitro, *FASEB J.*, 1991, **5**, 2860–2867.
119 S. Swasdison and R. Mayne, Formation of highly organized skeletal muscle fibers in vitro, *J. Cell Sci.*, 1992, **102**, 643–652.
120 T. Okano and T. Matsuda, Tissue engineered skeletal muscle: preparation of highly dense, highly oriented hybrid muscular tissues, *Cell Transplant.*, 1998, **7**, 71–82.
121 W. Bian, B. Liau, N. Badie and N. Bursac, Mesoscopic hydrogel molding to control the 3D geometry of bioartificial muscle tissues, *Nat. Protoc.*, 2009, **4**, 1522–1534.
122 J. Shansky, J. Chromiak, M. D. Tatto and H. Vandenburgh, A simplified method for tissue engineering skeletal muscle organoids in vitro, *In Vitro Cell. Dev. Biol.*, 1997, **33**, 659–661.
123 Y. Yamamoto, *et al.*, Preparation of artificial skeletal muscle tissues by a magnetic force-based tissue engineering technique, *J. Biosci. Bioeng.*, 2009, **108**, 538–543.
124 H. Vandenburgh, *et al.*, Automated drug screening with contractile muscle tissue engineered from dystrophic myoblasts, *FASEB J.*, 2009, **23**, 3325–3334.
125 H. Fujita, *et al.*, Fabrication of scaffold-free contractile skeletal muscle tissue using magnetite-incorporated myogenic C2C12 cells, *J. Tissue Eng. Regener. Med.*, 2010, **4**, 437–443.
126 Y. Yamamoto, *et al.*, Functional evaluation of artificial skeletal muscle tissue constructs fabricated by a magnetic force-based tissue engineering technique, *Tissue Eng., Part A*, 2011, **17**, 107–114.
127 H. Herr and R. G. Dennis, A swimming robot actuated by living muscle tissue, *J. Neuroeng. Rehabil.*, 2004, **1**, 6.
128 E. S. Boyden, F. Zhang, E. Bamberg, G. Nagel and K. Deisseroth, Millisecond-timescale, genetically targeted optical control of neural activity, *Nat. Neurosci.*, 2005, **8**, 1263–1268.
129 B. R. Arenkiel, *et al.*, In vivo light-induced activation of neural circuitry in transgenic mice expressing channelrhodopsin-2, *Neuron*, 2007, **54**, 205–218.
130 H. Wang, *et al.*, High-speed mapping of synaptic connectivity using photostimulation in channelrhodopsin-2 transgenic mice, *Proc. Natl. Acad. Sci. U. S. A.*, 2007, **104**, 8143–8148.
131 K. Deisseroth, Optogenetics, *Nat. Methods*, 2011, **8**, 26–29.
132 T. Bruegmann, *et al.*, Optogenetic control of heart muscle in vitro and in vivo, *Nat. Methods*, 2010, **7**, 897–900.
133 B. Arrenberg, D. Y. Stainier, H. Baier and J. Huisken, Optogenetic control of cardiac function, *Science*, 2010, **330**, 971–974.
134 T. Asano, T. Ishizua and H. Yawo, Optically controlled contraction of photosensitive skeletal muscle cells, *Biotechnol. Bioeng.*, 2012, **109**, 199–204.
135 M. S. Sakar, *et al.*, Formation and optogenetic control of engineered 3D skeletal muscle bioactuators, *Lab Chip*, 2012, **12**, 4976–4985.
136 M. Das, *et al.*, Embryonic motoneuron-skeletal muscle co-culture in a defined system, *Neuroscience*, 2007, **146**, 481–488.
137 Y. Morimoto, M. Neghishi-Kato, H. Onoe and S. Takeuchi, Three-dimensional neuron-muscle constructs with neuromuscular junctions, *Biomaterials*, 2013, **34**, 9413–9419.
138 J. A. Umbach, K. L. Adams, C. B. Gundersen and B. G. Novitch, Functional neuromuscular junctions formed by embryonic stem cell-derived motor neurons, *PLoS One*, 2012, **7**, e36049.

139 T. Kubo, M. A. Randolph, A. Gröger and J. M. Winograd, Embryonic stem cell-derived motor neurons form neuromuscular junctions in vitro and enhance motor functional recovery in vivo, *Plast. Reconstr. Surg.*, 2009, **123**, 139S–148S.
140 K. Kabumoto, T. Hoshino, Y. Akiyama and K. Morishima, Voluntary movement controlled by the surface EMG signal for tissue-engineered skeletal muscle on a gripping tool, *Tissue Eng., Part A*, 2013, **19**, 1695–1703.
141 Y. Akiyama, K. Iwabuchi, Y. Furukawa and K. Morishima, Electrical stimulation of cultured lepidopteran dorsal vessel tissue: an experiment for development of bioactuators, *In Vitro Cell. Dev. Biol.: Anim.*, 2010, **46**, 411–415.
142 Y. Akiyama, T. Hoshino, K. Iwabuchi and K. Morishima, Room temperature operable autonomously moving biomicrorobot powered by insect dorsal vessel tissue, *PLoS One*, 2012, **7**, e38274.

